

Communication

# Plasmonic Conglobation of Ultrathin Ag Nanofilms Far below Their Melting Points by Infrared Illumination

Han Dai <sup>1,2,\*</sup>, Junfeng Zhao <sup>1,\*</sup>, Tongjian Huang <sup>2</sup>, Xinxiang Yu <sup>1,2</sup>, Jie Sun <sup>1</sup>, Hongjie Fang <sup>1</sup>, Zhenfeng Zhu <sup>1</sup>, Mingfu Zhang <sup>3</sup> and Kun Yu <sup>1</sup>

<sup>1</sup> Laboratory of Composite Materials, Yantai Nanshan University, Longkou 265713, China; yuxinxiangcn@163.com (X.Y.); sunjie19860304@163.com (J.S.); h.j.fang@163.com (H.F.); zzfxcw951324@163.com (Z.Z.); yukun2010@csu.edu.cn (K.Y.)

<sup>2</sup> Shandong Nanshan Aluminum co. LTD. Longkou 264006, China; huangtongjian@nanshan.com.cn

<sup>3</sup> Guizhou University of Engineering Science, Bijie 551700, China; zhangmingfu\_163@163.com

\* Correspondence: daihan1985@189.cn (H.D.); zhaojunfengcc@163.com (J.Z.); Tel.: +86-15376985468 (H.D.); +86-13578724791 (J.Z.)

Received: 2 May 2018; Accepted: 23 May 2018; Published: 30 May 2018



**Abstract:** Plasmon heating has been employed as a low-temperature annealing method for the conglobation of ultrathin Ag nanofilms into nanoparticles both on silicon and carbon spheres, with complex surface structures, simply under illumination with infrared light. Finite-difference time-domain results provide evidence that the plasmonic light enhancements in the films' gaps and voids, rather than random surface fluctuations, are the main reason for the conglobation of Ag nanofilms far below the melting point of Ag. This technology can be applied in modern organic optoelectronic devices and photothermal pharma projects to reduce the thermal damage to materials or biological tissues.

**Keywords:** thin films; plasmonics; photothermal effects; nanomaterials

## 1. Introduction

Ag nanoparticles with significant light-harvesting and photothermal properties have attracted a lot of attention in recent years [1]. A lot of researchers have focused on the application of Ag nanoparticles for light management in optoelectronic devices [2,3] and for photothermal synergy therapies to treat cancer [4,5]. Recently, heat-labile organic or organic-inorganic hybrid materials, such as poly (3,4-ethylenedioxythiophene):polystyrene sulfonate (PEDOT:PSS), perovskites and pro-injected organic drugs in nanostructures have been used to improve the efficiency of optoelectronic devices [6,7] and pharma projects [8]. Spin coating [9], doctor blading [10] and screen printing [11] have been used to deposit metal nanoparticles on these heat-labile substrates without causing heat generation or introducing impurities. However, it is still challenging to use the above-mentioned coating methods owing to the low adhesion forces and the inhomogeneous distributions found on such substrate surfaces owing to their complex topological structures.

Plasmonic heating can occur in the nanoscale gaps, that is, at the grain boundaries; this generates extremely localized hot spots and causes atomic mass diffusion between the gaps [12,13]. Thus, plasmonic heating has been used as a new low-temperature welding technique for metal materials with one-dimensional nanostructures, for example, plasmonic welding for Ag or Cu nanowire networks [14,15]. Significant plasmonic heating can also be excited in two- or three-dimensional metal nanostructures as these have low melting points because of their enhanced surface energy [16]. However,

plasmonic heating for ultrathin metal nanofilms or other three-dimensional metal nanostructures has seldom been studied or applied.

In this work, we studied plasmonic heating for ultrathin Ag nanofilms and applied the technique for the fabrication of Ag nanoparticles on the surfaces of substrates with complex topological structures. Finite-difference time-domain (FDTD) results show that the plasmonic enhancement mainly occurs in the gaps or voids of the Ag nanofilms, rather than because of random surface fluctuations. The observation of the enlargement of the voids and rewelding of the Ag nanoparticles provides direct evidence for the plasmon-assisted conglomeration of Ag nanofilms. Owing to the highly localized plasmonic heat generation, the average temperature of the Ag nanofilm is far below its melting point when the conglomeration occurs. Therefore, the results of this study show great potential for the use of plasmonic heat generation in the fabrication of heat-labile organic or organic–inorganic hybrids in solar cells, light-emitting diodes or cancer pharma projects.

## 2. Materials and Methods

One-sided polished p-type Si (100) wafers with thicknesses of around 0.5 mm and carbon spheres were employed. Carbon spheres with smooth and porous surfaces were fabricated via hydrothermal synthesis. Specifically, 0.2 g polyvinylpyrrolidone powder, 15 mL ethylene glycol, and 5 mL HCl sol was mixed and autoclaved at 160 °C for either 14 or 22 h. Ultrathin Ag nanofilms were fabricated via low-temperature magnetron sputtering. The sputtering of the Ag nanofilms on silicon and carbon spheres was completed by using a turbo-pumped sputter coater (Q150TS, Quorum, Laughton, UK). All sputtering processes were sustained for 30 s with a sputtering current ranging between 10 and 40 mA to control the thickness of the Ag nanofilms on the substrates. Further, the above specimens were exposed to a near-infrared lamp (LP23030-B, Zhongjingkeyi Technology Co., Ltd., Beijing, China) with good tissue-penetration abilities to generate cytotoxic heat to destroy tumor cells. The power density of the lamp was approximately 10 W/cm<sup>2</sup>, and all specimens were illuminated for 15 min. During light illumination, the surface temperature of the Ag nanofilms gradually increased to 120–140 °C. The specimens were characterized using scanning electron microscopy (SEM) (JSM-6700F, JEOL Corp., Tokyo, Japan).

## 3. Results

Because of the poor wettability of Ag nanofilms on silicon substrates, a large number of voids and gaps exist in the ultrathin Ag nanofilms created using physical sputtering fabrication methods, and thus the photothermal effects can be relatively large [17]. As shown in Figure 1a,b, Ag nanofilms with a large number of voids and gaps segregated and conglobated together within a short time period (about 15 min) under light illumination. Reference test samples covered with Al foil (thickness 1 mm) are provided in the insets framed by the yellow dotted line. The Al foil-covered samples here can reflect the light and maintain a similar temperature as the samples under light illumination. Interestingly, the conglobations of Ag nanofilms with thicknesses below 10 nm display mutual bonding under light that is different from the characteristics of the sample under the cover. As a result, the average particle size of the Ag nanoparticles counted using ImageJ were much larger than without the light illumination when the thickness of the Ag nanofilms was below 10 nm, as shown in Figure 2a,b. As the thickness of the Ag nanofilm was increased to 20 nm, the light-induced conglomeration of the Ag nanofilms exhibited an increase in the size of the voids and gaps in the sample. As shown in Figure 1c, the conglomeration of the Ag nanofilms occurs at the voids and gaps—the light-induced conglomeration is much larger than that induced only with the heat treatment in the reference tests. The results show clearly that the energy provided by the light illumination is not sufficient for the thorough conglomeration of the Ag nanofilms into Ag nanoparticles on the silicon substrate when the thickness of the Ag nanofilms was increased to 20 nm. When the thickness was further increased to 30 nm, the Ag nanofilms became continuous films, with few voids or gaps observable. As shown in Figure 1d, few distinct conglobations occur on the 30-nm-thick Ag nanofilms via either light illumination or heat treatment below 140 °C.

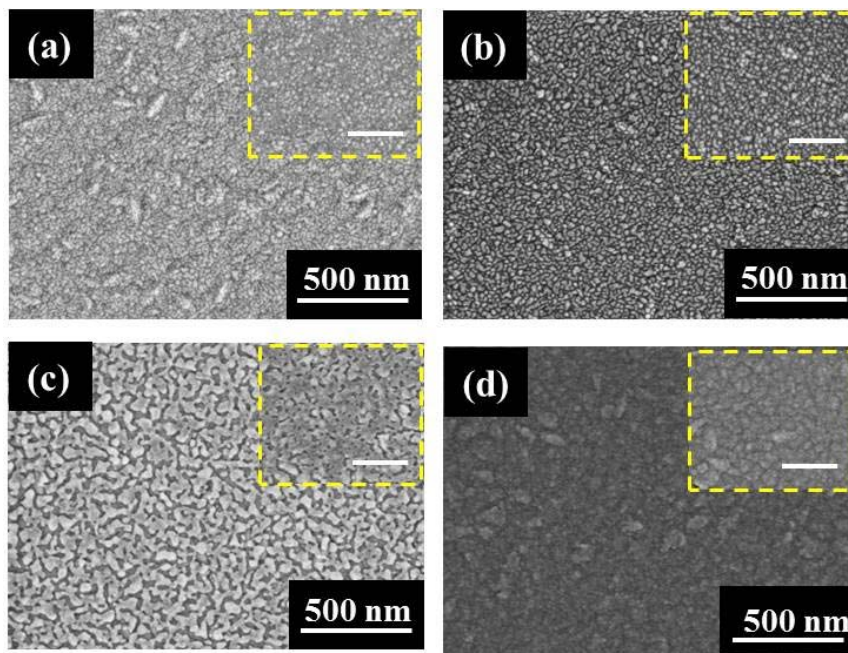


**Figure 1.** Conglobation of Ag nanofilms with various thicknesses with and without light illumination; (a–d) Ag nanofilms with thickness 5 nm, 10 nm, 20 nm and 30 nm, respectively, under light and under Al foil covers (insets). The scale bar in the inset is 250 nm.

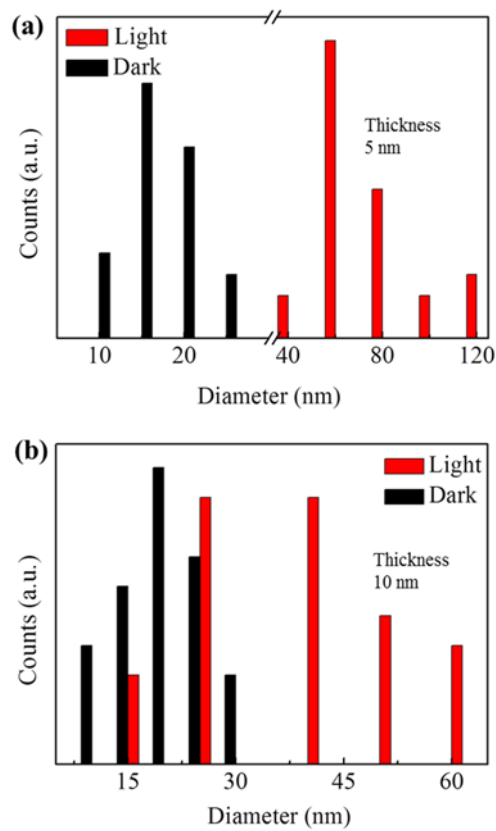


**Figure 2.** Statistical results of the diameters of Ag nanoparticles generated by Ag nanofilms with and without light illumination; (a) Ag nanofilms with thickness 5 nm; (b) Ag nanofilms with thickness 10 nm.

From a thermodynamics perspective, the conglomeration of metallic materials far below their melting points  $T_m$  can be primarily attributed to atomic diffusion [18]. The atomic diffusion temperature called Tamman temperature  $T_{tm}$  is only about  $0.3 T_m$  [19]. Meanwhile, the melting points of the nanoparticles and nanofilms will decrease along with their size [20]. The surface energy of Ag nanofilms increases as their thickness is reduced, which reduces the energy barrier and leads to surface atomic diffusion [21]. As shown in Figure 3, atomic diffusion in Ag nanofilms with 5 nm thickness generally requires a temperature of 230 °C, which is much higher than the surface temperature of the specimens in our case.

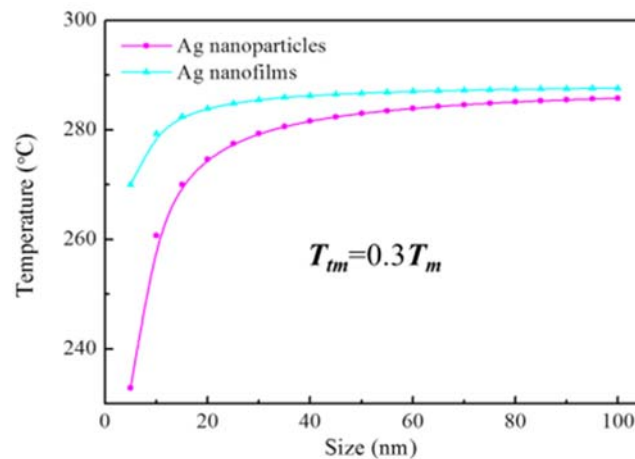


**Figure 3.** Tamman temperature of Ag nanoparticles and Ag nanofilms.

To further understand such thickness-dependent light-induced conglomeration, a model based on FDTD method was used to study the light enhancement of Ag nanofilms on silicon substrates. Herein, surface gap and void structures in Ag nanofilms at different depths were used to simulate actual grain boundaries (gaps) and holes (voids) in ultrathin Ag nanofilms under light illumination. The incident light adopted in this case was a plane wave with a wavelength of 800 nm that vertically illuminated the Ag nanofilms. According to the experimental results, a large number of voids exist when the thickness of the Ag nanofilms was reduced to 10 nm. Voids in the Ag nanofilms increased in size as the thickness of the Ag nanofilms was decreased, as shown in Figure 4a. Accordingly, light in the voids and gaps at different depths in the Ag nanofilms are presented in Figure 4c,d. Significant light enhancement can be observed in the voids and gaps in the Ag nanofilms. Additionally, the optical density enhancement in the voids is much higher than that in the gaps. Owing to the significant absorbance of Ag nanofilms, localized heat can be generated in these voids and gaps, causing the atoms to shift in these voids and gaps. A schematic diagram is presented in Figure 4b to illustrate the evolution of the transformation of the voids and gaps into Ag nanoparticles. The gaps grow into voids and the Ag nanofilms separate into small pieces; then, the small pieces conglobate into Ag nanoparticles because of their high surface energies. For the thicker Ag nanofilms with thicknesses larger than 30 nm, few voids are observed; these films are continuous. Therefore, light is rarely enhanced in these nanofilms, as shown in Figure 4e,f. Meanwhile, the surface energy of the Ag nanofilms is greatly reduced as the thickness is increased. As a result, surface conglomeration can barely be observed for Ag nanofilms with thicknesses of 30 nm. It should be noted that the effects of surface fluctuations on the Ag nanofilms were also been studied using FDTD. However, the surface fluctuations cannot couple light into the highly localized surface plasmons on the ultrathin Ag nanofilms because of the films' irregular morphologies, as shown in Figure 4g,h. Therefore, plasmonic enhancements in the void and gap structures are likely the main reason for the conglomeration of Ag nanofilms.

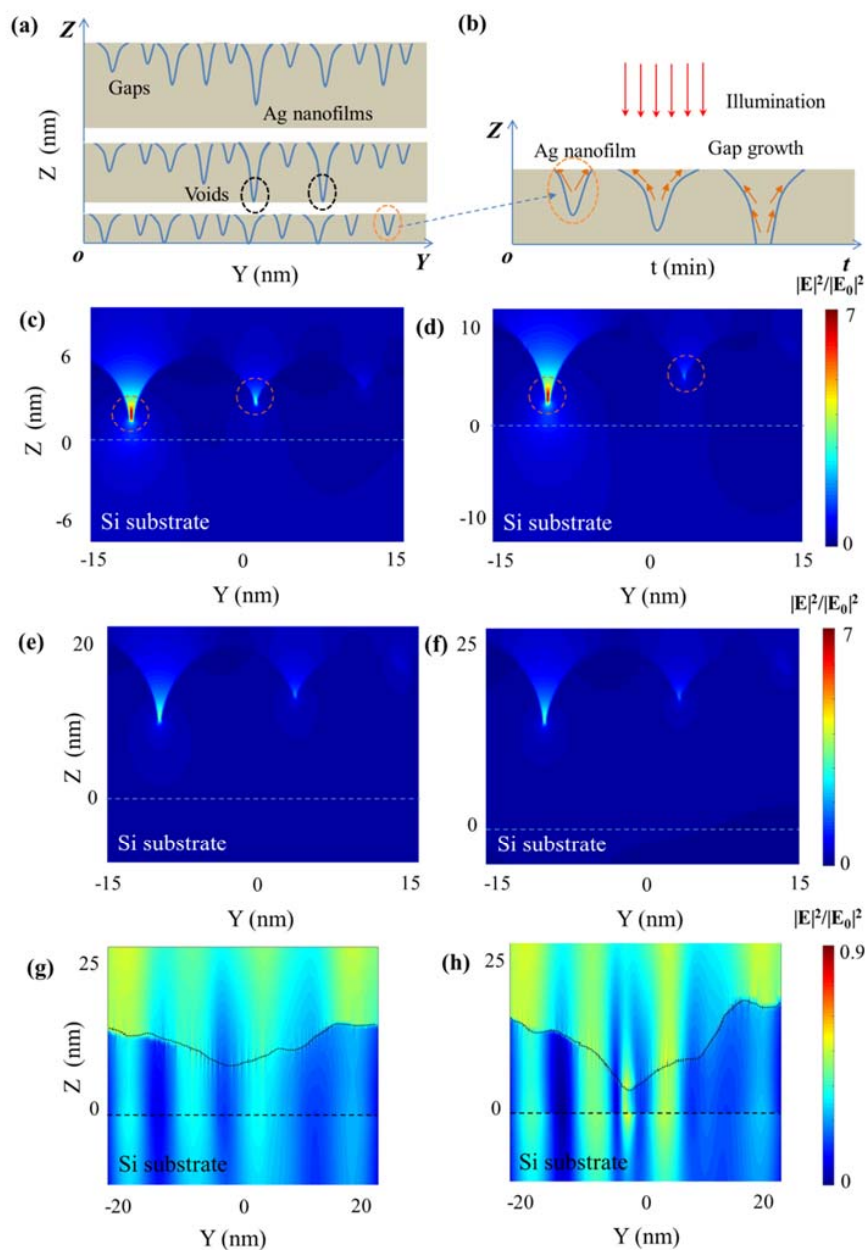


**Figure 4.** Voids induced plasmonic enhancement on Ag nanofilms with various thicknesses; (a) schematic diagram of voids in Ag nanofilms with various thicknesses; (b) schematic diagram of the evolution of gaps/voids in Ag nanofilms with light illumination; (c–f) plasmonic enhancement of gaps/voids on Ag nanofilms with 6 nm, 10 nm, 20 nm and 25 thicknesses; (g), (h) plasmonic enhancement of surface fluctuations on Ag nanofilms (thickness 10 nm) with average  $\pm 2$  nm and  $\pm 4$  nm.

When the Ag nanoparticles conglobate from the Ag nanofilms, plasmonic enhancement occurs at the interfaces, as shown in Figure 5a. Analogous to Ostwald ripening, small Ag nanoparticles can merge together with the assistance of plasmonic heating at the interfaces because of the nanoparticles' low  $T_m$  values, as shown in Figure 2. As the merging process proceeds, the plasmonic enhancement at the interfaces gradually reduces and finally causes the Ag nanoparticles to cease merging, as shown in Figure 5b. The plasmonic enhancement-assisted merging process of the Ag nanoparticles is also presented in a schematic diagram in Figure 5c. Compared with only the heat treatment, plasmonic heating yields Ag nanoparticles with larger particle sizes for Ag nanofilms with similar thicknesses.

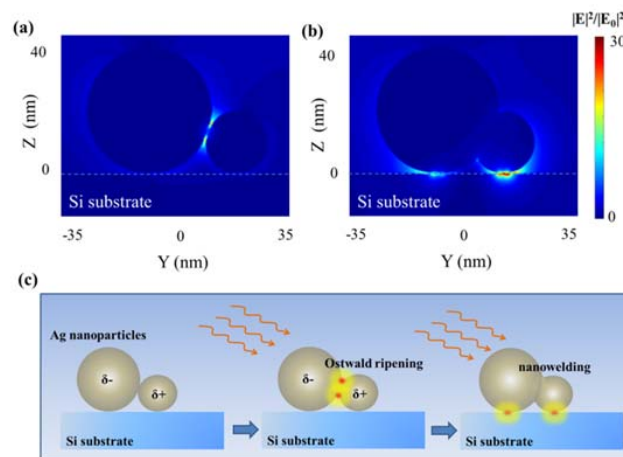


**Figure 5.** Plasmonic welding of Ag nanoparticles; (a) light enhancement of Ag nanoparticles (diameters 40 nm and 20 nm) in contact; (b) light enhancement of merged Ag nanoparticles; (c) schematic diagram of the plasmonic nanowelding of Ag nanoparticles.

To demonstrate the practicality of the conglomeration process for use with the complex topological structures presented by carbon spheres, carbon sphere samples with smooth and porous surfaces were first deposited before sputter coating 20-nm-thick Ag nanofilms on top. Carbon spheres and their core-shell structures with noble-metal nanoparticles have a broad range of applications in fields such as drug delivery [22], hydrogen storage [23], biodiagnostics [24] and photothermal conversion [25]. After 15 min of light illumination, the Ag nanofilms fully and uniformly segregated, forming nanoparticles with average diameters of about 30 nm on the top of both the carbon sphere samples with smooth and with porous surfaces, as shown in Figure 6a–f. The ambient temperature of the specimen was lower than 140 °C, which is far below the melting points of the Ag nanofilms. Note that this is significant as it demonstrates a light-induced “opening mechanism” (that is, a way to enlarge gaps in the Ag nanofilms) for Ag nanofilms coated on the carbon spheres (carbon sphere@Ag nanoparticle nanostructures) carrying, for example, drugs. Meanwhile, carbon sphere@Ag nanoparticle nanostructures exhibit remarkable photothermal properties [26]. Therefore, the light-conglomeration method has exciting potential applications in targeted drug transport and photothermal therapy for cancer.

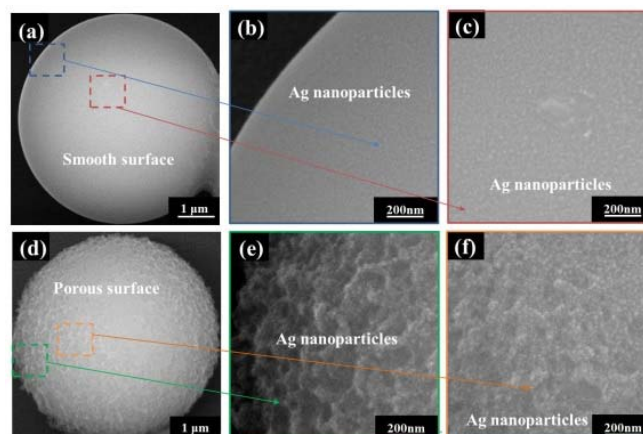


**Figure 6.** Light-induced conglomeration of Ag nanofilms on carbon spheres with smooth and porous surfaces. (a) Low-magnification image of Ag nanoparticles on carbon spheres with smooth surfaces; (b,c) surface morphologies of carbon sphere in the margin and center; (d) low-magnification image of Ag nanoparticles on carbon spheres with smooth surfaces; (e,f) surface morphologies of carbon sphere in the margin and center.

#### 4. Conclusions

In summary, we have reported a low-temperature conglomeration method for transforming Ag nanofilms into nanoparticles on silicon and carbon surfaces with temperatures much lower than the nanofilms' melting points by utilizing light illumination. Additionally, significant merging between the Ag nanoparticles was found with light illumination. Our FDTD results show that the low-temperature conglomeration of Ag nanofilms is mainly caused by plasmonic enhancement in the gap and void nanostructures in the Ag nanofilms. A straightforward application of our work is presented in the form of the fabrication of carbon spheres@Ag nanofilm composite structures. The design of these carbon spheres@Ag nanofilm composite structures highlights that this light-conglomeration method could have potential applications in optoelectronics and in the medical field.

**Author Contributions:** Conceptualization, H.D.; Methodology, J.Z.; Software, J.Z.; Validation, J.Z.; Formal Analysis, T.H.; Investigation, X.Y.; Resources, J.S.; Data Curation, H.F.; Writing-Original Draft Preparation, H.D.; Writing-Review & Editing, H.D.; Visualization, Z.Z.; Supervision, M.Z.; Project Administration, H.D.; Funding Acquisition, K.Y.

**Funding:** This research was funded by (A Project of Shandong Province Higher Educational Science and Technology Program) grant number (J17KA043, J17KB076); (Natural science foundation of Shandong province, China) grant number (ZR2017PEM005); (The natural science research project of the Guizhou provincial education department, China) grant number (KY2015472).

**Acknowledgments:** This research was supported by (The financial support of the 2015 ShanDong province project of outstanding subject talent group).

**Conflicts of Interest:** The authors declare no conflict of interest.

#### References

1. Franzen, S.; Folmer, J.C.W.; And, W.R.G.; O'Neal, R. Optical properties of dye molecules adsorbed on single gold and silver nanoparticles. *J. Phys. Chem. A* **2002**, *106*, 6533–6540. [[CrossRef](#)]
2. Lu, L.; Luo, Z.; Xu, T.; Yu, L. Cooperative plasmonic effect of Ag and Au nanoparticles on enhancing performance of polymer solar cells. *Nano Lett.* **2013**, *13*, 59–64. [[CrossRef](#)] [[PubMed](#)]
3. Shim, J.P.; Kim, D.; Choe, M.; Lee, T.; Park, S.J.; Lee, D.S. A self-assembled Ag nanoparticle agglomeration process on graphene for enhanced light output in GaN-based LEDs. *Nanotechnology* **2012**, *23*, 255201. [[CrossRef](#)] [[PubMed](#)]
4. Xu, R.; Ma, J.; Sun, X.; Chen, Z.; Jiang, X.; Guo, Z.; Huang, L.; Li, Y.; Wang, M.; Wang, C.; et al. Ag nanoparticles sensitize IR-induced killing of cancer cells. *Cell Res.* **2009**, *19*, 1031–1304. [[CrossRef](#)] [[PubMed](#)]
5. Foldbjerg, R.; Dang, D.A.; Autrup, H. Cytotoxicity and genotoxicity of silver nanoparticles in the human lung cancer cell line, A549. *Arch. Toxicol.* **2011**, *85*, 743–750. [[CrossRef](#)] [[PubMed](#)]
6. Wang, S.J.; Choi, Y.J.; Park, H.H. Investigation of Ag-poly(3,4-ethylenedioxythiophene):polystyrene sulfonate nanocomposite films prepared by a one-step aqueous method. *J. Appl. Phys.* **2011**, *109*, 124902. [[CrossRef](#)]
7. Jeon, N.J.; Noh, J.H.; Kim, Y.C.; Yang, W.S.; Ryu, S.; Seok, S.I. Solvent engineering for high-performance inorganic-organic hybrid perovskite solar cells. *Nat. Mater.* **2014**, *13*, 897–903. [[CrossRef](#)] [[PubMed](#)]
8. Wu, W.; Zhou, T.; Berliner, A.; Banerjee, P.; Zhou, S. Smart core-shell hybrid nanogels with Ag nanoparticle core for cancer cell imaging and gel shell for PH-regulated drug delivery. *Chem. Mater.* **2010**, *22*, 1966–1976. [[CrossRef](#)]
9. Norrman, K.; Ghanbari-Siahkali, A.; Larsen, N.B. Studies of spin-coated polymer films. *Annu. Rep. Prog. Chem. Sect. C* **2005**, *101*, 174–201. [[CrossRef](#)]
10. Schilinsky, P.; Waldauf, C.; Brabec, C. Performance analysis of printed bulk heterojunction solar cells. *Adv. Funct. Mater.* **2010**, *16*, 1669–1672. [[CrossRef](#)]
11. Krebs, F.C. Fabrication and processing of polymer solar cells: A review of printing and coating techniques. *Sol. Energy Mater. Sol. Cells* **2009**, *93*, 394–412. [[CrossRef](#)]
12. Garnett, E.C.; Cai, W.; Cha, J.J.; Mahmood, F.; Connor, S.T.; Greyson, C.M.; Yi, C.; McGehee, M.D.; Brongersma, M.L. Self-limited plasmonic welding of silver nanowire junctions. *Nat. Mater.* **2012**, *11*, 241–249. [[CrossRef](#)] [[PubMed](#)]

13. Ward, D.R.; Hüser, F.; Pauly, F.; Cuevas, J.C.; Natelson, D. Optical rectification and field enhancement in a plasmonic nanogap. *Nat. Nanotechnol.* **2010**, *5*, 732–736. [[CrossRef](#)] [[PubMed](#)]
14. Park, J.H.; Hwang, G.T.; Kim, S.; Seo, J.; Park, H.J.; Yu, K.; Kim, T.S.; Lee, K.J. Flash-induced self-limited plasmonic welding of silver nanowire network for transparent flexible energy harvester. *Adv. Mater.* **2017**, *29*, 1603473. [[CrossRef](#)] [[PubMed](#)]
15. Park, J.H.; Han, S.; Kim, D.; You, B.K.; Joe, D.J.; Hong, S.; Seo, J.; Kwon, J.; Jeong, C.K.; Park, H.J.; et al. Plasmonic-tuned flash Cu nanowelding with ultrafast photochemical-reducing and interlocking on flexible plastics. *Adv. Funct. Mater.* **2017**, *27*, 1701138. [[CrossRef](#)]
16. Stark, W.J.; Stoessel, P.R.; Wohlleben, W.; Hafner, A. Industrial applications of nanoparticles. *Chem. Soc. Rev.* **2015**, *44*, 5793–5805. [[CrossRef](#)] [[PubMed](#)]
17. Teo, E.J.; Toyoda, N.; Yang, C.; Wang, B.; Zhang, N.; Bettiol, A.A.; Teng, J.H. Sub-30 nm thick plasmonic films and structures with ultralow loss. *Nanoscale* **2014**, *6*, 3243–3249. [[CrossRef](#)] [[PubMed](#)]
18. Taylor, A.B.; Siddiquee, A.M.; Chon, J.W. Below melting point photothermal reshaping of single gold nanorods driven by surface diffusion. *ACS Nano* **2014**, *8*, 12071–12079. [[CrossRef](#)] [[PubMed](#)]
19. Takaishi, T.; Saito, M.J. Effect of pretreatment on the 2-dimensional condensation of adsorbed krypton on alkali chlorides. *Phys. Chem.* **1967**, *71*, 453–454. [[CrossRef](#)]
20. Nanda, K.K.; Sahu, S.N.; Behera, S.N. Liquid-drop model for the size-dependent melting of low-dimensional systems. *Phys. Rev. A* **2002**, *66*, 013208. [[CrossRef](#)]
21. Lu, Y.; Huang, J.Y.; Wang, C.; Sun, S.; Lou, J. Cold welding of ultrathin gold nanowires. *Nat. Nanotechnol.* **2010**, *5*, 218–224. [[CrossRef](#)] [[PubMed](#)]
22. Liu, J.; Wickramaratne, N.P.; Qiao, S.Z.; Jaroniec, M. Molecular-based design and emerging applications of nanoporous carbon spheres. *Nat. Mater.* **2015**, *14*, 763–774. [[CrossRef](#)] [[PubMed](#)]
23. Ströbel, R.; Garche, J.; Moseley, P.T.; Jörissen, L.; Wolf, G. Hydrogen storage by carbon materials. *J. Power Sources* **2006**, *159*, 781–801. [[CrossRef](#)]
24. Liu, S.; Wang, X.; Zhao, H.; Cai, W. Micro/nano-scaled carbon spheres based on hydrothermal carbonization of agarose. *Colloids Surf. A Physicochem. Eng. Asp.* **2015**, *484*, 386–393. [[CrossRef](#)]
25. Lu, A.H.; Zhang, X.Q.; Sun, Q.; Zhang, Y.; Song, Q.; Schüth, F.; Cheng, F. Precise synthesis of discrete and dispersible carbon-protected magnetic nanoparticles for efficient magnetic resonance imaging and photothermal therapy. *Nano Res.* **2016**, *9*, 1460–1469. [[CrossRef](#)]
26. Li, D.; Han, D.; Qu, S.N.; Liu, L.; Jing, P.T.; Zhou, D.; Ji, W.Y.; Wang, X.Y.; Zhang, T.F.; Shen, D.Z. Supra-(carbon nanodots) with a strong visible to near-infrared absorption band and efficient photothermal conversion. *Light Sci. Appl.* **2016**, *5*, e16120. [[CrossRef](#)]

